Polymeric nitrogen

C. Mailhiot, L. H. Yang, and A. K. McMahan

Lawrence Livermore National Laboratory, University of California, Livermore, California 94551
(Received 22 April 1992; revised manuscript received 23 June 1992)

The equilibrium phase boundary between single-bonded, threefold-coordinated polymeric forms of nitrogen, and the observed, triple-bonded diatomic phases, is predicted to occur at relatively low (50 ± 15 GPa) pressure. This conclusion is based on extensive local-density-functional total-energy calculations for polymeric structures (including that of black phosphorus, and another with all *gauche* dihedral angles) and diatomic structures (including that of the observed high-pressure ε-N_2 phase). We believe the diatomic phase of nitrogen, observed up to 180 GPa and room temperature, to be metastable at these conditions, and that such hysteresis enhances the prospects for the existence of a metastable polymeric form of nitrogen at ambient conditions. In this regard, we show that the black-phosphorus and cubic *gauche* polymeric forms of nitrogen would encounter significant barriers along high-symmetry paths to dimerization at atmospheric pressure.

I. INTRODUCTION

All known solid phases of nitrogen assume a diatomic molecular form,[1] characterized by strong triple covalent bonds ($N\equiv N$) within each N_2 molecule, and weak van der Waals interactions between different molecules.[2] Nitrogen is the only group V element that assumes this form in its condensed phases, "in preference to polymerizing to single-bonded systems as in the case of phosphorus and arsenic."[2] It is the purpose of this paper to report *ab initio* pseudopotential total-energy calculations which suggest, however, that such polymeric forms of nitrogen may exist in the bulk, both as thermodynamically stable phases at high pressure, and as metastable phases at atmospheric pressure.

There has been recent interest by chemists in finite counterparts of polymeric nitrogen phases, i.e., large N_n molecules bound by single (N—N) or single and double (N=N) bonds, as potential energetic materials.[3-9] Theoretical calculations have focused on a hypothetical N_4 analogue of observed P_4,[3] on a N_6 analogue of benzene as well as other N_6 isomers,[3-7] and on a N_8 analogue of cubane.[8] There are also studies on N_3H_3 isomers, in which the nitrogens are singly or doubly bound to one another.[9] While the calculations suggest that many of these hypothetical molecules should be metastable, i.e., exhibit real vibrational frequencies, there has been as yet no conclusive experimental evidence as to their existence. There are, however, indications that N_6 may have been observed,[10] and perhaps N_3H_3 as well.[11]

There is also considerable interest within the high-pressure physics community in the possible existence of bulk polymeric phases of nitrogen. It is generally expected that the application of sufficient pressure must eventually destroy covalent bonds in solids, and in particular lead to the dissociation of diatomic bonds in molecular solids.[12] Such dissociation in solid iodine has been well documented,[13] and that in solid hydrogen is the object of

considerable current interest.[14] Nitrogen offers an additional complication because of the N_2 triple bond, which contrasts with the single bonds present in I_2 and H_2. The essential conclusion that may be drawn from previous theoretical work on high-pressure nitrogen phases is that the $N\equiv N$ triple bond will be destabilized at lower pressures than the N—N single bond.[15-17] That is, nitrogen should transform from its ambient diatomic form to an intermediate, still covalent, polymeric regime before losing its covalency altogether at still higher pressures. Two calculations[15,16] have placed the transition to the polymeric regime at pressures below 100 GPa (100 GPa $\equiv$ 1 Mbar), the lower estimate being at 70 GPa.[16] Subsequent diamond-anvil-cell experiments to 130 and 180 GPa, however, indicate that nitrogen remains diatomic to these pressures at room temperature, this conclusion being based on the fact that only modest changes were observed in the measured intramolecular vibron frequency.[18,19] It may simply be that the diatomic phase is itself metastable at these pressures, since, for example, the graphite to diamond transition in carbon must be overdriven by about a factor of 7 in pressure even at a temperature of 1000 K.[20] On the other hand, an anomaly has been observed above 30 GPa in hot shock compressed fluid nitrogen,[21] and has been interpreted as the occurrence of dissociation to a dense atomic phase.[22] This interpretation is consistent with the theoretically predicted phase transition at low temperatures.[23]

In this paper, we present extensive *ab initio* pseudopotential total-energy results for both polymeric and diatomic phases of nitrogen, which not only reaffirm the previous theoretical conclusions, but suggest that an even lower pressure of $\sim$50 GPa is the more likely phase boundary above which *stable* nitrogen phases at low temperature should be polymeric. This reduction follows from our identification of a polymeric form of nitrogen, characterized by all *gauche* dihedral angles, which has a significantly lower (0.86 eV/atom) total energy than pre-

viously considered polymeric forms. At the same time we report *ab initio* pseudopotential total-energy calculations for the observed high-pressure ε-N_2 diatomic phase. We also provide estimates of the local-density-functional errors in this diatomic equation of state, based on comparisons with experimental data. While our local-density-functional predictions indicate a 33-GPa transition from the ε-N_2 phase to the new polymeric form of nitrogen, these considerations lead to what we believe to be a realistic 50 ± 15 GPa placement of the diatomic-polymeric phase boundary for solid nitrogen at low temperatures.

The single-bonded group-V elements exhibit structures that are generally related to simple cubic (sc). This structure is itself observed at high pressure in both phosphorus and arsenic, and a rhombohedral distortion ($A7$) is the ambient phase of arsenic, antimony, and bismuth, and is also seen at pressures below the sc phase in phosphorus.[1] The two previous theoretical upper bounds on the transition pressure from diatomic to polymeric nitrogen assumed these two structures (sc and $A7$) for the polymeric phase,[15,16] with the lower 70 GPa result associated with the lower-energy $A7$ structure.[16] The ambient black-phosphorus (BP) phase of phosphorus,[1] an orthorhombic distortion of sc, is another natural candidate structure to consider for a polymeric form of nitrogen. We report here *ab initio* total-energy calculations for nitrogen in the BP structure, and find indeed a total energy which is 0.28 eV/atom lower at equilibrium (pressure $p = 0$) than that of $A7$ nitrogen. Moreover, the relative energy ordering of these $A7$ and BP curves for nitrogen is also consistent with dependence of the total energy on the dihedral angle in N_2X_4 (i.e., X_2N–NX_2) molecules.[24] This correspondence has led us to consider a "cubic *gauche*" (cg) distortion of sc, in which we find nitrogen to have an equilibrium total energy a further 0.58 eV/atom below that of the BP structure. It is to this hypothetical cg phase of polymeric nitrogen that we find a transition from the diatomic form at 50 ± 15 GPa.

The location of the low-temperature equilibrium phase boundary between diatomic and polymeric forms of nitrogen also depends crucially on the calculated equation of state for the diatomic phase. While the structure of nitrogen is unknown above about 20 GPa, there exist strong indications from Raman data that all phases of nitrogen so far observed at pressures over 10 GPa are closely related to the δ-N_2 ($Pm\bar{3}n$) structure.[1] In particular, the ε-N_2 ($R\bar{3}c$) phase observed at cryogenic temperatures from 1.9 to about 20 GPa is a slight rhombohedral distortion of the δ-N_2 structure due in part to orientational ordering of the N_2 molecules.[25,26] Raman data suggest a further lowering of symmetry (possibly $R3c$) at about 20 GPa.[25] We report in this paper *ab initio* local-density-functional calculations of the observed ε-N_2 structure.[27] For comparison, we also report calculations for diatomic nitrogen in two other structures which are characteristic of slightly prolate molecules,[28] namely, the α-N_2 ($Pa\bar{3}$) and β-O_2 ($R\bar{3}m$) structures. While we find the ε-N_2 structure to have the lowest energy of the three at high pressure, as expected, the more important conclusion is that the differences in energy are relatively small in the vicinity of 50 GPa. We therefore conclude that un-

certainties in the precise structure of the diatomic phase in this pressure range have relatively small impact on our location of the equilibrium diatomic-polymeric phase boundary. Larger uncertainties for the diatomic phase are due to local-density-functional errors in the treatment of the intermolecular van der Waals interactions. However, by a comparison to experimental data for both diatomic nitrogen and similarly van der Waals bonded solid argon, we believe we have relatively good estimates of these errors, which are included in our predicted 50 ± 15 GPa location of the diatomic-polymeric phase boundary.

We suggest that the room-temperature diatomic phase of nitrogen, observed[18,19] at pressures approximately three times higher than our calculated equilibrium phase boundary, must be metastable at these conditions. If diatomic nitrogen exhibits such large hysteresis, which is common for covalent solids,[20] polymeric forms stable above $\sim$50 GPa may well also be metastable at atmospheric pressure. To investigate this question, we also consider high-symmetry transformation paths by which the BP and cg polymeric forms might dimerize at atmospheric pressure ($p \sim 0$), and also some paths between the various polymeric forms. In all cases we find that bond breaking or at least significant bond bending is required along these paths, and in all cases we find significant barriers as, for example, a $\sim$0.9 eV/atom barrier inhibiting dimerization of the atmospheric-pressure cg phase. While these results are far from conclusive, they are consistent with the possibility that each of the $A7$, BP, and cg phases of nitrogen may be mechanically stable at atmospheric pressure.

In the remainder of this paper, Sec. II gives a description of the total-energy methods and of the *ab initio* pseudopotential for nitrogen used in the present work. After characterization of the various structures, our total-energy results as a function of atomic volume are presented in Sec. III for the polymeric and diatomic phases of nitrogen, as well as for a number of higher-coordination metallic phases. Our predicted location of the polymeric-diatomic phase boundary is also given in this section. Section IV presents our $p = 0$ metastability analysis for the three ($A7$, BP, and cg) polymeric structures, and our conclusions are given in Sec. V.

II. THEORETICAL METHOD

The results presented below were obtained using *ab initio* pseudopotentials implemented with a plane-wave basis for the expansion of the electronic wave functions. Nitrogen is an element for which a pseudopotential description should be adequate because the core $1s^2$ states do not overlap significantly with the valence states. However, since the core of nitrogen consists only of $1s^2$ states, there is no cancellation for the p and d states in the core region and, consequently, the resulting pseudopotentials are very attractive for these angular momentum channels. Consequently, a large number of plane waves are required to provide a correct description of the nitrogen pseudowave function.

The pseudopotential calculations whose results are presented below are performed within the frame-

work of local-density-functional theory[29] applied in the momentum-space formalism.[30,31] We use nonlocal, norm-conserving,[32] ab initio ionic pseudopotentials generated in a separable form.[33] A procedure recently suggested by Trouiller and Martins[34] to generate soft, nonlocal, ab initio pseudopotentials was adopted. The Ceperley-Alder[35] model is used for the exchange-correlation potential, as parametrized by Perdew and Zunger.[36] In addition to the total energy E, the pressure p and the forces are calculated analytically from the stress theorem.[37] Brillouin zone summations are performed using sets of special k points generated using the Monkhorst-Pack algorithm.[38,39] A kinetic energy cutoff of $E_{cutoff} = 80$ Ry was used to calculate the total energy for all the structures and transformation paths. To treat the large set of plane waves resulting from this large E_{cutoff}, we used the local optimization scheme of Teter, Payne, and Allan.[40]

III. TOTAL ENERGIES OF STRUCTURES

The results of our ab initio total-energy calculations are presented below. Given the large number of structures considered, we organize our presentation by discussing, in turn, metallic, polymeric, and diatomic phases. When describing the various structures, we follow standard crystallographic notation[41] by defining vectors (x, y, z) in terms of the conventional unit cell vectors a, b, and c:

$$(x, y, z) \equiv x\mathbf{a} + y\mathbf{b} + z\mathbf{c}. \tag{1}$$

We then use this notation to list both the subset of site positions associated with the primitive cell, and also the three primitive cell vectors $\mathbf{a}_0$, $\mathbf{b}_0$, and $\mathbf{c}_0$.

A. Metallic phases

The structures of the metallic phases considered here are well known and need not be described. Our calculated results for the total energy per atom as a function of atomic volume are shown in Fig. 1 for the face-centered-cubic (fcc), ideal $(c/a = \sqrt{8/3})$ hexagonal close-packed (hcp), body-centered-cubic (bcc), cubic diamond (cd), and simple cubic (sc) structures. Values of the equilibrium $(p = 0)$ atomic volume V_0, bulk modulus B_0, and total energy E_0 for these metallic phases were obtained by fitting the calculated total energies to Murnaghan's equation of state[42] and are indicated in Table I. Our results are in excellent correspondence with those obtained from previous linear muffin-tin orbitals[15] and ab initio pseudopotential[16] analyses which confirm the accuracy of our soft nonlocal pseudopotential.

The half-filled $2p^3$ shell of nitrogen tends to favor crystal structures in which bonds are oriented approximately along the lobes of the p_x, p_y, and p_z orbitals in orthogonal directions.[43] This is suggestive of the sc structure which may be considered prototypical of the group-V elemental solids. Indeed, heavier group-V elements exhibit atmospheric-pressure phases which are distortions of the sc structure, while the sc structure itself is actually ob-

served at high pressure in both phosphorus and arsenic. Inspection of Fig. 1 and Table I reveals that the six-fold coordinated sc phase has substantially lower energy than the high-coordination (8 and 12) bcc, fcc, and hcp metals, and that its equilibrium energy is even slightly lower than fourfold coordinated cd, which is also metallic in the case of nitrogen. This behavior anticipates the fact that further significant reductions in total energy arise from distortions of the sc structure which split its six near-neighbor distances into three first-nearest- and three second-nearest-neighbor distances. Such distorted-sc structures exhibit the threefold coordination which is ideally suited to the capacity for each nitrogen atom to form three covalent bonds. We refer to these structures as polymeric in contrast to the triple bonds within the N_2 molecules of the diatomic phases.

B. Polymeric threefold-coordinated phases

We now consider threefold-coordinated polymeric forms of nitrogen. These include the arsenic ($A7$), black-phosphorus (BP), and cubic gauche (cg) phases, whose structural characterization is given in Table II. The $A7$ and BP structures are natural candidates for polymeric forms of nitrogen, as they are observed phases of other group-V elemental solids. The arsenic $A7$ structure consists of a rhombohedral distortion of the sc phase and
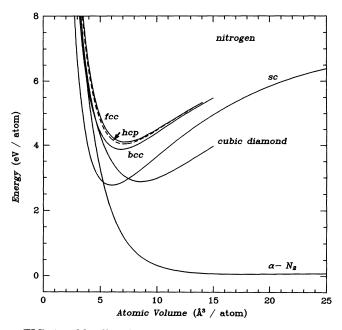

FIG. 1. Metallic phases of nitrogen. Calculated total energy per atom for the face-centered-cubic (fcc), ideal hexagonal close-packed (hcp, dashed curve) with $(c/a) = \sqrt{8/3}$, body-centered-cubic (bcc), simple-cubic (sc), and cubic diamond (cd) phases of nitrogen as a function of atomic volume. A kinetic energy cutoff of $E_{cutoff} = 80$ Ry was used to calculate the total energy for all the structures. The number of k points used for the calculations was fcc (28), hcp (36), bcc (26), sc (20), and cd (28). The zero of energy corresponds to the minimum energy of the diatomic α-N_2 ($Pa\bar{3}$) phase, which is discussed in Sec. III D, and included here for comparison.

TABLE I. Ground-state properties of nitrogen phases. Metallic phases include the face-centered-cubic (fcc), ideal hexagonal close-packed (hcp), body-centered-cubic (bcc), cubic diamond (cd), and simple-cubic (sc) structures. Polymeric phases (see Table II) include the arsenic ($A7$), black-phosphorus (BP), trans-cis chain (ch), and cubic gauche (cg) structures. Diatomic phases (see Table III) include the β-O_2 and α-N_2 structures. All calculations were performed with a kinetic energy cutoff of 80 Ry. The values of the equilibrium ($p = 0$) atomic volume V_0, bulk modulus B_0, and total energy E_0 were obtained by fitting the calculated total energies to Murnaghan's equation of state. Energies are given relative to that of our α-N_2 ($Pa\bar{3}$) structure at its equilibrium volume. Experimental data for this low-temperature diatomic form of nitrogen are given for comparison.

Structure	V_0 (Å^3/atom)	B_0 (GPa)	E_0 (eV/atom)
fcc	7.30	167.68	4.06
hcp	7.35	189.68	4.00
bcc	7.01	212.81	3.82
cd	8.62	213.83	2.81
sc	6.24	228.21	2.72
$A7$	6.49	259.63	1.83
BP	6.34	316.94	1.55
ch	10.24	162.98	1.24
cg	6.67	340.66	0.97
β-O_2	19.67	2.20	0.02
α-N_2	18.50	7.47	0.00
α-N_2 (expt[a])	21.67[b]	2.16	

[a]T. A. Scott, Phys. Rep. **27**, 89 (1976).
[b]A 3.6% zero-point volume expansion has been removed. See Ref. 27.

is the atmospheric-pressure form exhibited by antimony, bismuth, and arsenic itself. The pressure sequence $A7$ → sc is observed in As at room temperature.[44,45] The BP structure is an orthorhombic distortion of sc, and is the observed atmospheric-pressure form of phosphorus. Phosphorus is known to exhibit the structural transformation sequence BP → $A7$ → sc under pressure.[46,47] After discussing our theoretical results for the $A7$ and BP phases, we indicate how these two phases exhibit local geometric relationships similar to those found in small N_2X_4 molecules of the form X_2N-NX_2. This correspondence between our optimized results for nitrogen in the $A7$ and BP structures and small molecules led us to consider a third topology which we refer to as "cubic gauche" (cg), which is then discussed. The cg phase was found to be the lowest-energy polymeric form of nitrogen among the candidate structures considered here.

The arsenic $A7$ structure belongs to the $R\bar{3}m$ space group, with a rhombohedral (trigonal) Bravais lattice, and two atoms per primitive cell. It corresponds to a distortion of the sc phase obtained by a strain of the sc unit cell along the [111] direction and a simultaneous displacement of the atoms of the basis towards each other in pairs in the same direction. The distortion from sc is typically large enough so that the $A7$ structure is layer-like, as is evident in the schematic illustration indicated in Fig. 2. The hexagonal unit cell vectors defined by Table II are

$$\mathbf{a} = a_{A7}\,\hat{\mathbf{x}}\,, \tag{2a}$$

$$\mathbf{b} = a_{A7}\,(-\hat{\mathbf{x}} + \sqrt{3}\,\hat{\mathbf{y}})/2\,, \tag{2b}$$

$$\mathbf{c} = c_{A7}\,\hat{\mathbf{z}}\,. \tag{2c}$$

TABLE II. Structural characterization of theoretically calculated polymeric phases of nitrogen at atmospheric pressure. The name (abbreviation) is given for each structure, along with the space group, the magnitudes a, b, c of the unit cell vectors, the unit cell multiplicities and Wyckoff site letters, and the corresponding dimensionless internal parameters x, y, z. Hexagonal axes are used for rhombohedral $R\bar{3}m$. The bond lengths, dihedral angles, and bond angles are specified for each structure. Multiple entries indicate proportions, e.g., two-thirds of the BP bonds have lengths equal to 1.54 Å.

Structure	Space group[a]	a, b, c (Å)	Sites[a]	x, y, z	Bond length(s) (Å)	Dihedral angle(s) (deg)	Bond angle(s) (deg)
Arsenic ($A7$)	$R\bar{3}m$ 166	2.401	6c		1.59	180.0	97.8
		7.803		0.217			
Black phos-	$Cmca$	2.299	8f		1.53	180.0	96.2
phorus (BP)	64	7.268		0.10	1.54	+76.0	102.2
		3.036		0.08	1.54	−76.0	102.2
Cubic gauche (cg)	$I2_13$ 199	3.765	8a	0.085	1.40	−106.8	114.0
Trans-cis chain (ch)	$Cmcm$ 63	2.616	8f		1.24	180.0	106.0
		8.272		0.072	1.55	0.0	
		3.787		0.045			

[a]Reference 41.

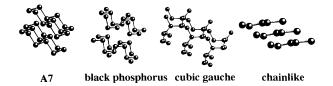A7   black phosphorus   cubic gauche   chainlike

FIG. 2. *Polymeric phases of nitrogen.* Schematic representation of threefold-coordinated arsenic ($A7$), black-phosphorus (BP), and cubic *gauche* (cg) phases, and of a twofold-coordinated chainlike (ch) phase.

In terms of these, the two c positions associated with the primitive cell are

$$\pm(0,\, 0,\, z_{A7})\,, \tag{3}$$

while the three primitive cell vectors are

$$\mathbf{a}_0,\, \mathbf{b}_0,\, \mathbf{c}_0 \;=\; (-\tfrac{2}{3},\, -\tfrac{1}{3},\, \tfrac{1}{3}),\; (\tfrac{1}{3},\, -\tfrac{1}{3},\, \tfrac{1}{3}),\; (\tfrac{1}{3},\, \tfrac{2}{3},\, \tfrac{1}{3})\,. \tag{4}$$

It is evident that the $A7$ structure is completely determined by a specification of the independent structural parameters a_{A7}, c_{A7}, and z_{A7}. The sc structure corresponds to the special case where $(c/a)_{A7} = \sqrt{6}$ and $z_{A7} = \tfrac{1}{4}$.

The BP phase corresponds to the $Cmca$ space group, with an end- or C-centered orthorhombic Bravais lattice, and four atoms per primitive cell. It is also a layered structure as seen in Fig. 2, however, the corrugated double layers develop perpendicular to the [100] sc directions, in contrast to the [111] directions in the case of $A7$. The unit cell vectors defined by Table II are $\mathbf{a} = a_{BP}\,\hat{\mathbf{x}}$, $\mathbf{b} = b_{BP}\,\hat{\mathbf{y}}$, and $\mathbf{c} = c_{BP}\,\hat{\mathbf{z}}$. In terms of these, the four f positions associated with the primitive cell are

$$\pm(0, y_{BP}, z_{BP}),\quad \pm(0, \tfrac{1}{2}+y_{BP}, \tfrac{1}{2}-z_{BP}), \tag{5}$$

while one possible choice for the primitive cell vectors is

$$\mathbf{a}_0,\, \mathbf{b}_0,\, \mathbf{c}_0 \;=\; (1,0,0),\; (\tfrac{1}{2},\tfrac{1}{2},0),\; (0,0,1)\,. \tag{6}$$

The BP structure is uniquely specified by a knowledge of the five independent structural parameters a_{BP}, b_{BP}, c_{BP}, y_{BP}, and z_{BP}. A sc-like limit for the individual double layers is obtained for $(c/a)_{BP} = 1$, $(yb/a)_{BP} = 1/\sqrt{8}$, and $z_{BP} = 0$. However, adjacent double layers appear shifted by $\tfrac{1}{2}\mathbf{a}$ relative to one another in this limit, and a monoclinic path is required to actually reach the sc structure, e.g., the $4e$ sites of $P2_1/c$.

The results of our total-energy *ab initio* pseudopotential calculations for the $A7$ and BP threefold coordinated polymeric phases of nitrogen are presented in Fig. 3, where the calculated total energy per atom is shown as a function of atomic volume, and in Tables I and II, where equilibrium bulk and structural properties are given, respectively. The c/a ratio was optimized at every volume for the $A7$ unit cell, with the zero-pressure value $(c/a)_{A7} = 3.25$, which is somewhat larger than previously found on the basis of pseudopotential calculations.[16] The internal parameter z_{A7} was set to $z_{A7} = 0.217$ in accordance with previous analyses[16] of the $A7$ phase of ni-

trogen. Full optimization of the internal parameter is expected to result in small second-order effects on the value of the total energy. Both (b/a) and (c/a) ratios were fully optimized for the BP unit cell near zero pressure; however, these equilibrium ratios were then used for calculations at all other volumes. Except as specifically indicated, the internal parameters for the BP phase of nitrogen were fixed at their corresponding known values in phosphorus:[48] $y_{BP} = 0.10$ and $z_{BP} = 0.08$. The equilibrium atomic volume V_0, bulk modulus B_0, and total energy E_0 for the $A7$ and BP phases were obtained from Murnaghan fits as in the case of the metallic phases, and are indicated in Table I; and the corresponding optimized lattice constants, in Table II. Our results for the $A7$ structure of nitrogen are in good correspondence with *ab initio* pseudopotential[16] analyses which have appeared in the literature for this phase. We are not aware of any previous theoretical analyses for comparison in the case of the BP structure, however.

One set of test calculations was carried out for the BP structure with internal parameters different from those in Table II. The choice was motivated by the 96.2° bond angle for BP in this table, which is somewhat smaller than N$-$N bond angles typically found in small molecules.[2] As a sensitivity analysis, we considered setting *all* bond angles equal to 102.2°, while retaining the same bond lengths as in Table II. The choice of these parameters requires $a_{BP} = 2.405$ Å, $(b/a)_{BP} = 3.022$, $(c/a)_{BP} = 1.236$, $y_{BP} = 0.099$, and $z_{BP} = 0.087$. We then carried out total-energy calculations as a function of volume with the lattice-constant ratios and internal parameters fixed at these new values. The resulting curve is quite similar to the BP result shown in Fig. 3, although shifted to $\sim$10% larger volumes, and reduced slightly (0.03 eV/atom) in equilibrium energy. The corresponding equilibrium quantities are $V_0 = 7.32$ Å^3/atom, $B_0 = 212.35$ GPa, and $E_0 = 1.52$ eV/atom. The differences between these results and those given in Fig. 3 and Tables I and II are sufficiently small that we have chosen to report the latter results, obtained with $y_{BP} = 0.10$ and $z_{BP} = 0.08$, for which complete optimization of the lattice-constant ratios was carried out at equilibrium.

The essential result indicated by Fig. 3 is that distortion of the metallic high-coordination sc phase to threefold coordinated polymeric structures causes substantial lowering of the energy with respect to the sc structure: by 0.89 eV/atom for the sc $\rightarrow$ $A7$ distortion and 1.17 eV/atom for the sc $\rightarrow$ BP distortion. This behavior is not unexpected: Previous calculations[16] have indeed indicated that the $A7$ was a lower-energy phase than the sc structure (0.56 eV/atom as reported in Ref. 16), and the possibility of polymerization to a threefold-coordinated BP phase has also been previously suggested.[15] However, our results constitute a prediction, on the basis of *ab initio* total-energy calculations, of the existence of a nitrogen BP phase exhibiting lower energy than the arseniclike $A7$ structure.

We now discuss an analogy between small N_2X_4 molecules and our hypothetical polymeric phases ($A7$ and BP) of nitrogen which has lead us to consider yet another polymeric form of nitrogen, a "cubic *gauche*" (cg) struc-

ture, which exhibits all-*gauche* helicity. Isomers of N_2X_4 stoichiometry arranged in X_2N-NX_2 configurations can be characterized by a dihedral angle ϕ, defined as the angle by which one of the X_2N groups must be rotated about the axis of the N—N bond in order to be located precisely above (i.e., eclipse) the other NX_2 group.[2] It is believed that the juxtaposition of the lone-pair electrons on each of the two nitrogens has significant impact on the preferred value of ϕ,[24] so that the optimal ϕ may, to a first approximation, be viewed as a property of the N—N bond, independent of the attached X_2 group. Results of quantum chemistry calculations[24] reveal common features of the energy curves $E(\phi)$ as a function of the dihedral angle ϕ: These curves tend to exhibit an absolute maximum at the *cis* ($\phi = 0°$) conformation, absolute minima at *gauche* ($\phi = \pm67°$ for N_2F_4 and $\phi = \pm91°$ for N_2H_4) conformations, and a local minimum at the *trans* ($\phi = 180°$) conformation.[24] The local bonding topology associated with the $A7$ and BP structures can also be described in terms of such dihedral angles. The $A7$ structure is seen in Table II to be pure *trans*, while the BP structure has one-third of its bonds *trans*, and two-thirds *gauche* (equal numbers $\phi = +76°$ and $-76°$). Since the equilibrium BP energy in Table I is 0.28 eV/atom lower than that of the $A7$ structure, an obvious possibility, considering the small-molecule trends discussed above, is that an all-*gauche* structure might have lower energy yet. If one connects a sc array of sites using only three bonds per site *and* ensures that all such bonds have the same dihedral angle (for example, all $-90°$), one arrives at the cubic space group $I2_13$.

The cg structure belongs to the $I2_13$ space group, with a body-centered-cubic Bravais lattice, and four atoms per primitive cell. Unlike the $A7$ and BP distortions of sc, where the covalent bonds form corrugated double layers which are van der Waals bound to other such double layers, the cg structure is truly a three-dimensional covalent network, in that every atom is linked to every other atom by a continuous path of covalent bonds. A schematic representation of the cg structure is indicated in Fig. 2. The unit cell vectors in terms of the parameters in Table II are $\mathbf{a} = a_{cg}\,\hat{\mathbf{x}}$, $\mathbf{b} = a_{cg}\,\hat{\mathbf{y}}$, and $\mathbf{c} = a_{cg}\,\hat{\mathbf{z}}$. In terms of these, the four a sites associated with the primitive cell are

$$(x_{cg}, x_{cg}, x_{cg}), \quad (\tfrac{1}{2}-x_{cg}, -x_{cg}, \tfrac{1}{2}+x_{cg}),$$

$$(-x_{cg}, \tfrac{1}{2}+x_{cg}, \tfrac{1}{2}-x_{cg}), \quad (\tfrac{1}{2}+x_{cg}, \tfrac{1}{2}-x_{cg}, -x_{cg}), \tag{7}$$

while the customary primitive cell vectors are

$$\mathbf{a}_0, \ \mathbf{b}_0, \ \mathbf{c}_0 \ = \ (-\tfrac{1}{2},\tfrac{1}{2},\tfrac{1}{2}), \ (\tfrac{1}{2},-\tfrac{1}{2},\tfrac{1}{2}), \ (\tfrac{1}{2},\tfrac{1}{2},-\tfrac{1}{2}) \ . \tag{8}$$

The cg structure reduces to sc for $x_{cg} = 0$. The cg structure exhibits threefold coordination with all bonds of equal length given by

$$d_{cg} \ = \ 2a_{cg}\sqrt{x_{cg}^2 + \left(x_{cg} - \tfrac{1}{4}\right)^2} \ , \tag{9}$$

and similarly all bond angles of equal value given by

$$\cos\theta_{cg} \ = \ \frac{x_{cg}(x_{cg} - \tfrac{1}{4})}{x_{cg}^2 + (x_{cg} - \tfrac{1}{4})^2} \ . \tag{10}$$

The structure is completely defined by a specification of the parameters a_{cg} and x_{cg} which permit the realization of any bond length d_{cg} and bond angle θ_{cg}. However, the unique dihedral angle ϕ_{cg},

$$\sec(\phi_{cg}) \ = \ \sec(\theta_{cg}) - 1 \ , \tag{11}$$

is completely determined by the bond angle for this structure, and vice versa.

The results of our total-energy *ab initio* pseudopotential calculations for the cg threefold-coordinated polymeric phase of nitrogen are shown in Fig. 3, where the calculated total energy per atom is indicated as a function of atomic volume. Extensive total-energy calculations were performed to determine the lattice constant a_{cg} and internal parameter x_{cg} yielding minimum-energy configurations at vanishing pressure and forces. These structural parameters are provided in Table II, and the corresponding values of the equilibrium atomic volume V_0, bulk modulus B_0, and total energy E_0 are indicated in Table I. To give some idea of the sensitivity of the energetics to x_{cg}, the value $x_{cg} = 0.048$ leads to an equilibrium energy $E_0 = 1.57$ eV/atom, bond length $d_{cg} = 1.54$
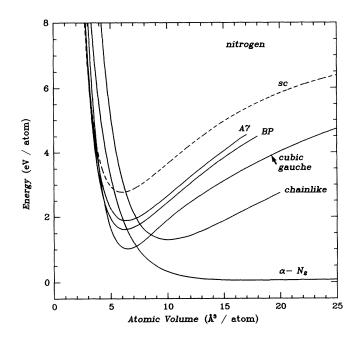

FIG. 3. *Polymeric phases of nitrogen.* Calculated total energy per atom for the threefold-coordinated arsenic ($A7$), black-phosphorus (BP), and cubic *gauche* (cg) phases of nitrogen, and for a twofold-coordinated chainlike (ch) phase of nitrogen, as a function of atomic volume. A kinetic energy cutoff of $E_{cutoff} = 80$ Ry was used to calculate the total energy for all the structures. The number of $\mathbf{k}$ points used for the calculations was $A7$ (28), BP (16), cg (18), and ch (16). The zero of energy corresponds to the minimum energy of the diatomic α-N_2 ($Pa\bar{3}$) phase, which is discussed in Sec. III D. The simple-cubic (sc, dashed curve) phase is included here for comparison.

Å, and bond angle $\theta_{cg} = 103°$, which may be compared to the optimized values in the tables. Inspection of Fig. 3 and Table I reveals that the fully optimized polymeric cg phase is lower in energy than the BP structure (by 0.58 eV/atom) which is consistent with the trend exhibited by the small N_2X_4 molecules in regard to the preference of the N—N bond for *gauche* dihedral angles. More important, the polymeric cg structure is the lowest-energy atomic phase of nitrogen which has so far been found in any calculation, to our knowledge, and, as we discuss below, it has significant impact on predictions of the pressure-induced dissociation or polymerization of the ambient diatomic form of nitrogen

Finally, it is also worth comparing the bond lengths and bond angles of the equilibrium $A7$, BP, and cg structures in Table II to what is known from molecular systems. Although the calculated N—N bond length in the $A7$ structure is somewhat large, the BP and cg bond lengths agree well with the 1.45 ± 0.08 Å range observed for the single N—N bond in small molecules, especially compared to the length of a typical double (1.23 Å in N_2F_2) or triple (1.10 Å in N_2) bond.[2] Similarly, the bond angles in Table II lie within or close to the 100°–116° range of XNY bond angles encountered in small molecules where nitrogen forms single bonds.[2] In this regard, we have noted above that the equilibrium energy of the BP phase is very slightly reduced if the small 96.2° BP bond angle is increased to 102.2°.

C. Polymeric twofold-coordinated chainlike phases

We have also considered partially polymerized twofold coordinated chainlike structures where single (N—N) and double (N=N) bonds alternate. Within the confines of the present work, we restrict our analysis to only one simple example of such a structure. Our results in this case will hopefully provide an indication of the relative energetics of this class of partially polymerized chainlike phases in comparison to the fully polymerized threefold-coordinated phases, such as $A7$, BP, and cg, discussed above.

The hypothetical chainlike structure we have considered was motivated by the prevalence of planar $XN=NX$ molecules (e.g., where X is H, F, or CH_3) of both *trans* and *cis* conformations.[2] We thus take a planar chain (ch) of alternating *trans* and *cis* bonds of lengths characterized by a single bond angle. One may, in fact, distort (via the lower-symmetry $C222_1$ subgroup) the corrugated double layers of the BP structure so as to arrive at such chains pointing in the c direction. The resulting chainlike structure is described by the $Cmcm$ space group, with a C-centered orthorhombic Bravais lattice, and four atoms per primitive cell. A schematic representation is indicated in Fig. 2. The unit cell vectors defined by Table II are $\mathbf{a} = a_{ch}\,\hat{\mathbf{x}}$, $\mathbf{b} = b_{ch}\,\hat{\mathbf{y}}$, and $\mathbf{c} = c_{ch}\,\hat{\mathbf{z}}$. The four f positions associated with the primitive cell are

$$\pm(0, y_{ch}, z_{ch}), \quad \pm(0, y_{ch}, \tfrac{1}{2} - z_{ch}), \tag{12}$$

while the primitive cell vectors may be taken as

$$\mathbf{a}_0, \ \mathbf{b}_0, \ \mathbf{c}_0 \ = \ (1,0,0), \ (\tfrac{1}{2}, \tfrac{1}{2}, 0), \ (0,0,1) \ . \tag{13}$$

It is evident that the chain structure is uniquely specified by a knowledge of the three lattice constants (a_{ch}, b_{ch}, c_{ch}) and two internal parameters (y_{ch} and z_{ch}).

The results of our total-energy *ab initio* pseudopotential calculations for the hypothetical twofold-coordinated chainlike ($Cmcm$) phase of nitrogen are indicated in Fig. 3 where the calculated total energy per atom is given as a function of atomic volume. Only the lattice constant a_{ch} was varied, with fixed ratios $(b/a)_{ch} = 3.16$ and $(c/a)_{ch} = 1.45$, and similarly, fixed internal parameters $y_{ch} = 0.072$ and $z_{ch} = 0.045$. These values were chosen so that the c-direction chains would exhibit 106° bond angles (characteristic of FN=NF), and for one value of a_{ch}, the two different bond lengths would equal typical double (1.23 Å) and single (1.53 Å) nitrogen bond lengths, respectively, as seen in small molecules.[2] The ratio $(b/a)_{ch}$ was taken simply to be that of the equilibrium BP structure. It is evident from Table II that the minimum-energy structure as a function of a_{ch} does indeed yield bond lengths quite close to those adopted by small molecules. We also carried out similar calculations for internal parameters ($y_{ch} = 0.083$, $z_{ch} = 0.057$) which would allow more nearly equal bond lengths, taking in this case both ratios $(c/a)_{ch}$ and $(b/a)_{ch}$ to be the same as the BP equilibrium values. These results gave a curve very similar to that in Fig. 3, shifted to slightly smaller volumes. The equilibrium parameters were $V_0 = 8.99$ Å^3/atom, $B_0 = 176.35$ GPa, and $E_0 = 1.23$ eV/atom in this case.

In spite of the lack of optimization, there are important conclusions to be drawn from the comparison of the twofold-coordinated chainlike structure with the other results shown in Fig. 3. First, while it has a relatively low equilibrium total energy E_0, the ch curve appears shifted to higher volumes in Fig. 3, relative to the threefold coordinated polymeric phases. One consequence of this fact is that it never drops below any of the diatomic curves, raising the possibility that low-temperature diatomic nitrogen may transform under pressure directly to one of the threefold coordinated polymeric phases, without any intermediate regime of chainlike behavior. Secondly, at atomic volumes exceeding approximately 8.5 Å^3/atom, the chainlike structure has the lowest energy among the candidate polymeric phases considered here. Since this is the volume regime probed by high-temperature shock compression experiments, it is possible that the formation of chainlike nitrogen fragments may play a role in the anomaly observed in that data.[21–23]

D. Diatomic phases

Nitrogen at low temperature and atmospheric pressure is a diatomic molecular solid or liquid. Below 35.6 K, α-N_2 exhibits the cubic $Pa\bar{3}$ structure (4 N_2 molecules/cell) characterized by molecular axes oriented along the body diagonals of the cubic unit cell.[48,1] At low temperature and at a pressure of 0.35 GPa, the α-N_2 phase transforms into the tetragonal γ-N_2 characterized by the $P4_2/mnm$ space group (2 N_2 molecules/cell) with the N_2 molecules arranged in layers with a common orientation but with a shift of 90° between adjacent layers.[49] Raman data indi-

cate a structural transition at 1.9 GPa from tetragonal γ-N_2 ($P4_2/mnm$) to ε-N_2 which exhibits the rhombohedral $R\bar{3}c$ structure (8 N_2 molecules per primitive cell).[26] The ε-N_2 ($R\bar{3}c$) phase is known to persist up to 20 GPa above which pressure the structure of nitrogen is unknown, although it is likely to be a lower-symmetry distortion of the $R\bar{3}c$ structure.[27]

Because of our interest in the pressure-induced dissociation (or polymerization) of the observed diatomic form of nitrogen, the high pressure ε-N_2 ($R\bar{3}c$) phase is of particular importance to our transition-pressure calculations of the next subsection. Furthermore, while the diatomic structure is not precisely known above 20 GPa, we consider a selection of other diatomic structures characteristic of nearly spherical molecules like N_2 in order to get some sense of the uncertainties. In particular, we also carry out calculations here for the cubic α-N_2 ($Pa\bar{3}$) structure and the rhombohedral β ($R\bar{3}m$) structure (one molecule per primitive cell) observed for solid O_2. The structural data for each of the ε-N_2, α-N_2, and β-O_2 structures is given in Table III.

The low-temperature and pressure α-N_2 modification of nitrogen is described by space group $Pa\bar{3}$, with a simple-cubic Bravais lattice, and eight atoms (four molecules) per primitive cell. As noted above, the four N_2 molecules orient along the four cube body diagonals.[48,1] They undergo orientational librations as well as center-of-mass vibrations about their equilibrium positions.[1] The conventional unit cell described by Table III is primi-

tive, with $\mathbf{a}_0 = \mathbf{a} = a_{\alpha N_2}\,\hat{\mathbf{x}}$, $\mathbf{b}_0 = \mathbf{b} = a_{\alpha N_2}\,\hat{\mathbf{y}}$, and $\mathbf{c}_0 = \mathbf{c} = a_{\alpha N_2}\,\hat{\mathbf{z}}$. Four of the c sites are given by

$$(x_{\alpha N_2}, x_{\alpha N_2}, x_{\alpha N_2}),\quad (\tfrac{1}{2}-x_{\alpha N_2}, -x_{\alpha N_2}, \tfrac{1}{2}+x_{\alpha N_2}),$$
$$(-x_{\alpha N_2}, \tfrac{1}{2}+x_{\alpha N_2}, \tfrac{1}{2}-x_{\alpha N_2}),\qquad\qquad (14)$$
$$(\tfrac{1}{2}+x_{\alpha N_2}, \tfrac{1}{2}-x_{\alpha N_2}, -x_{\alpha N_2}),$$

with the remaining four (the other atomic site in each molecule) obtained by evaluating these same expressions with the N_2 bond length d in Table III replaced by $-d$, which for this structure just changes the sign of $x_{\alpha N_2}$. Clearly $x_{\alpha N_2} = 0$ gives the center-of-mass positions, which are seen to form a face-centered-cubic lattice.

The ε-N_2 ($R\bar{3}c$) phase is the observed low-temperature structure of nitrogen between 1.9 and 20 GPa. It is conveniently described in terms of the higher-temperature disordered cubic δ-N_2 structure which was first discovered at 300 K and 4.9 GPa.[50] The δ-N_2 phase has a disordered cubic structure with space group $Pm\bar{3}n$ and 8 N_2 molecules within the simple-cubic cell: There are six molecules with disklike disorder and two with spherical disorder. The δ-ε transition occurs through the orientational ordering and small displacement of the N_2 molecules, accompanied by a slight extension of the cubic unit cell along the cube diagonal, resulting in a rhombohedral cell characterized by a small reduction of the angle between the axes from 90° to approximately 85°.[50]

A detailed description of the ε-N_2 phase has appeared in the literature.[26,27] It corresponds to the space group

TABLE III. Structural characterization of theoretically calculated diatomic phases of nitrogen. The name is given for each structure, along with the space group, the ratios b/a and c/a of the magnitudes of the unit cell vectors, the unit cell multiplicities and Wyckoff site letters, and the corresponding dimensionless internal parameters x, y, z. Hexagonal axes are used for rhombohedral $R\bar{3}m$ and $R\bar{3}c$. The N_2 bond length was taken to be $d = 1.10$ Å.

Structure	Space group[a]	b/a	c/a	Sites[a]	x, y, z
α-N_2	$Pa\bar{3}$ 205	1	1	$8c$	$d/(2\sqrt{3}a)$
ε-N_2 [b]	$R\bar{3}c$ 167		1.3649	$12c$	
				$36f$	$d/(2c)$ $0.241 + 0.306\,d/c$ $0.241 - 0.306\,d/c$ $0.25 + 0.315\,d/c$
β-O_2	$R\bar{3}m$ 166		3.0	$6c$	$d/(2c)$
Two-layer β-O_2	$Cmcm$ 63	$\sqrt{3}$	2.0	$8f$	$\tfrac{1}{6}$ $0.25 - d/(2c)$

[a]Reference 41.
[b]References 26 and 27.

$R\bar{3}c$, with a rhombohedral (trigonal) Bravais lattice, and 16 atoms (8 molecules) per primitive cell. The hexagonal unit cell vectors presumed by Table III are the same as in Eq. (2), with substitution of the appropriate ε-N$_2$ lattice constants, and similarly the primitive vectors are given by Eq. (4). In terms of the unit cell vectors, the four (two molecules) c sites associated with the primitive cell are

$$(0,0,z_{\varepsilon N_2}^{(1)}), \quad (0,0,\tfrac{1}{2}+z_{\varepsilon N_2}^{(1)}), \tag{15a}$$

and the 12 (6 molecules) f sites associated with the primitive cell are

$$\begin{aligned}&\pm(x_{\varepsilon N_2}^{(2)}, \ y_{\varepsilon N_2}^{(2)}, \ z_{\varepsilon N_2}^{(2)}),\\ &\pm(-y_{\varepsilon N_2}^{(2)}, \ x_{\varepsilon N_2}^{(2)}-y_{\varepsilon N_2}^{(2)}, \ z_{\varepsilon N_2}^{(2)}),\\ &\pm(-x_{\varepsilon N_2}^{(2)}+y_{\varepsilon N_2}^{(2)}, \ -x_{\varepsilon N_2}^{(2)}, \ z_{\varepsilon N_2}^{(2)}),\end{aligned} \tag{15b}$$

where as before these expressions are to be evaluated using $\pm d$ in Table III to obtain the two atoms in each molecule. Note that the c and f sites are analogues of the "spherical" and "disklike" sites, respectively, in the high-temperature cubic δ-N$_2$ structure. The ε-N$_2$ structure is characterized by the six independent parameters, two lattice constants $(a_{\varepsilon N_2}, c_{\varepsilon N_2})$, and four internal parameters $(z_{\varepsilon N_2}^{(1)}, x_{\varepsilon N_2}^{(2)}, y_{\varepsilon N_2}^{(2)}, z_{\varepsilon N_2}^{(2)})$.

The β-O$_2$ structure with one N$_2$ molecule per primitive cell corresponds to exactly the same $R\bar{3}m$ space group and same set of site positions as the arsenic $A7$ structure described by Eqs. (2)–(4). The important difference is that the internal parameter $z_{\beta O_2} = d/(2c_{\beta O_2})$ is small for β-O$_2$, and is a measure of the diatomic bond length d, in contrast to $z_{A7} \sim \tfrac{1}{4}$. The diatomic β-O$_2$ structure can clearly be continuously transformed into the polymeric $A7$ structure by varying the internal structural parameter z. The β-O$_2$ structure may be viewed as closed-packed hexagonal planes of molecules, with the molecular axis aligned perpendicular to the planes stacked in the $\dots[ABC]\dots$ sequence characteristic of the fcc structure.[16] In our metastability calculations of Sec. IV, we also consider the hcp analogue, i.e., an $\dots[AB]\dots$ stacking sequence, described in Table III as the "two-layer β-O$_2$" structure. We emphasize that there is no evidence for the existence of a β-O$_2$ phase for diatomic nitrogen. However, it is useful to perform total-energy calculations for this structure observed in oxygen at low temperatures and pressures, since the N$_2$ and O$_2$ molecules exhibit similar degrees of prolateness,[28] and so the β-O$_2$ structure is not unreasonable to consider for diatomic nitrogen. Moreover, the ab initio total-energy results presented below for the β-O$_2$ phase of nitrogen can serve as the basis of a comparison with theoretical analyses reported earlier on this structure using similar methods.[16]

Results of our ab initio pseudopotential total-energy calculations for the α-N$_2$, ε-N$_2$, and β-O$_2$ phases of nitrogen are indicated in Fig. 4 where the calculated total energy per atom is shown as a function of atomic volume. For all calculations performed for the diatomic structures, the intramolecular N≡N bond length was fixed at the value $d = 1.10$ Å, extracted from an independent

FIG. 4. *Diatomic phases of nitrogen.* Calculated total energy per atom for the α-N$_2$ ($Pa\bar{3}$), ε-N$_2$ ($R\bar{3}c$), and β-O$_2$ ($R\bar{3}m$, dashed curve) diatomic phases of nitrogen as a function of atomic volume. A kinetic energy cutoff of $E_{\text{cutoff}} = 80$ Ry was used to calculate the total energy for all the structures. The number of k points used for the calculations was α-N$_2$ (11), ε-N$_2$ (2 and 10 in tests), and β-O$_2$ (10) The zero of energy corresponds to the minimum energy of the α-N$_2$ phase.
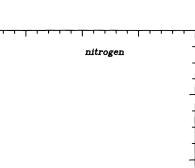
set of ab initio pseudopotential total-energy calculations performed for an isolated N$_2$ diatomic molecule. The calculated value of the N$_2$ intramolecular bond length $d^{\text{calc}} = 1.10$ Å is in perfect agreement with the experimental value $d^{\text{expt}} = 1.10$ Å.[2] The internal parameters in Table III defining the structure of the diatomic phases shown in Fig. 4 were therefore determined by requiring that $d = 1.10$ Å for all atomic volumes. For the cubic α-N$_2$ phase, this determination of d uniquely specifies the internal structural parameter $x_{\alpha N_2}$ as is indicated in Table III. In accordance with previous theoretical analyses of the ε-N$_2$ phase,[27,15] our ab initio total-energy calculations were performed with the rhombohedral angle $\alpha \equiv \cos^{-1}(\hat{a}_0 \cdot \hat{b}_0)$ fixed at the value $\alpha_{\varepsilon N_2} = 85.72°$, or equivalently $(c/a)_{\varepsilon N_2} = 1.3649$, and the internal parameters specifying the center of mass and the orientation of the N$_2$ molecules kept constant at the values theoretically determined for this structure at 75 GPa.[51] For the β-O$_2$ phase, a value of $(c/a)_{\beta O_2} = 3.0$ was adopted at all volumes. This value is close to that used in previous theoretical analyses[16] and we have not felt it necessary to perform extensive energy-minimum structural searches for the β-O$_2$ phase since it is not experimentally observed in nitrogen. Moreover, the structural parameter which affects the energy most significantly is the bond length d of the diatomic molecule.

Inspection of Fig. 4 reveals that our calculated ε-N$_2$ curve drops below that of the other two diatomic results as volume is decreased away from the right side of the fig-

ure, in qualitative agreement with experimental observations. The ε-N_2 phase continues to be the lowest-energy diatomic form in the range $V = 8$–9 Å^3/atom which will be crucial to our calculated dissociation or polymerization transition. Equally important is the fact that the differences in energy between the three diatomic phases considered here are relatively small (≤ 0.1 eV/atom) in this region. We take these differences to be a measure of that contribution to the uncertainty in our diatomic equation of state in this range which is due to our lack of knowledge of the true crystal structure. Specifically, we consider the possibility that the correct structure may have an energy ~ 0.1 eV/atom lower than that of our calculated ε-N_2 curve in the vicinity $V = 8$–9 Å^3/atom.

Another source of error in our diatomic results at large volume is evident in Table I, where values of the equilibrium ($p = 0$), atomic volume V_0, bulk modulus B_0, and total energy E_0 for the optimized α-N_2 and β-O_2 structures of N_2 are given. It may be seen that our calculated values of V_0 and B_0 for the α-N_2 structure are 15% smaller and 3.5 times larger, respectively, than the experimental values for this phase.[52] Such disagreement is characteristic of local-density approximation errors incurred at large volumes for van der Waals bonded materials. For example, in the case of solid fcc argon, local-density-functional calculations[53] yield values of V_0 and B_0 which are 21% smaller and 2.9 times larger, respectively, than experimental values.[1] A comparison to diamond-anvil-cell measurements,[54] however, shows a significant improvement in the theoretical volume (only 8% smaller than experiment) by a pressure of $p \sim 5B_0 \sim 14$ GPa. Thereafter, a more gradual improvement is seen, with the theoretical volume about 5% small by 80 GPa, the highest pressure reached in these experiments on argon.[54] We believe this same type of behavior is evident in the present results for the *diatomic* phases of nitrogen.

To quantify better the present uncertainties for our N_2 phases, a comparison between our calculated pressure for the ε-N_2 phase (solid curve labeled "ε-N_2") and the ~ 100 K data for this phase taken by Mills *et al.*[26] is indicated in Fig. 5. Our theoretical volume is about 10% and 9% smaller than experiment at the limits of this data, 6 and 13 GPa, respectively. This also is about a factor of 2 improvement by $p \sim 5B_0$ in comparison to the α-N_2 results at $p = 0$, as was the case with argon, and we expect analogous gradual improvement at higher pressures. The dashed curve in Fig. 5 is a semiempirical ε-N_2 equation of state from which we may extract a quantitative measure of the consequence of these local-density approximation, van der Waals errors on the dissociation or polymerization transition to be described in the next subsection. It is a Murnaghan fit to the data of Mills *et al.*[26] which is constrained to agree with theory at 500 GPa and, with the argon example in mind, to have a volume 5% larger than the local-density result near 80 GPa. Finally, the equation of state of the cg polymerized phase is also presented (solid curve labeled "cg-N") in Fig. 5 for comparison. It is to be emphasized that local-density-functional theory generally provides excellent equation of state results (volume errors <2%) for group-IV and -V fourfold
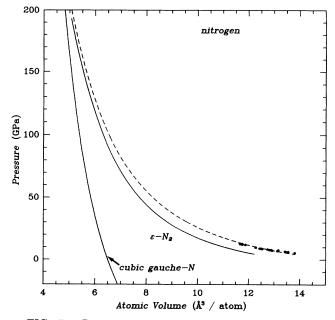

FIG. 5. *Pressure-volume equations of state.* The solid curves give the calculated pressure as a function of atomic volume for the polymeric cg-N and the diatomic ε-N_2 phases of nitrogen. The dashed curve is a semiempirical ε-N_2 equation of state constrained to agree with the theory at 500 GPa, and with the experimental data of Ref. 26 (data points) below 13 GPa.

and threefold-coordinated phases, and so we expect the primary uncertainties in the present numerical results to arise from the diatomic calculations.

E. Polymerization of nitrogen

The calculated equations of state for the polymeric (Fig. 3) and diatomic (Fig. 4) phases of nitrogen allow a determination of the transition pressure at which the N_2 molecules in diatomic solid nitrogen should dissociate, or more specifically, polymerize to a single-bonded threefold coordinated network. The transition pressure for the zero-temperature ε-$N_2 \rightarrow$ cg-N polymerization reaction is given by the slope of the common tangent to the diatomic and polymeric total-energy curves as a function of volume, as shown in Fig. 6, or equivalently by the crossing of the corresponding Gibbs free-energy curves as a function of pressure. Our results suggest the relatively low transition pressure of $p = 50 \pm 15$ GPa, above which a polymeric form of nitrogen should be the thermodynamically stable phase of nitrogen. However, because of the large barriers between diatomic and polymeric forms of nitrogen discussed in the next section, it may be necessary to overdrive this pressure significantly and/or heat the sample in order to observe the transition experimentally. We have noted that in room-temperature experiments, the diatomic form appears to be stable at pressures up to 180 GPa.[18,19] Because of this complication, it is important to establish clearly the theoretical uncertainties in order to rule out the possibility that the equilibrium phase boundary might occur at a signif-
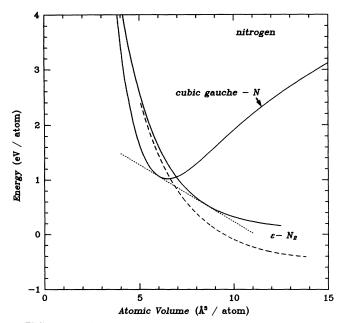
FIG. 6. *Polymerization of nitrogen.* The solid curves give the calculated total energy per atom for the polymeric cg-N and diatomic ε-N_2 phases of nitrogen as a function of atomic volume. The dashed curve is the semiempirical ε-N_2 total energy, corresponding to the dashed curve in Fig. 5. The common tangent to the two theoretical curves (dotted line) gives an ε-$N_2 \to$ cg-N transition pressure of 33 GPa, whereas substitution of the semiempirical result for ε-N_2 increases the pressure to 50 GPa.

icantly higher pressure than predicted. We believe our stated uncertainties to be realistic, and the focus of the discussion in this subsection is our determination of these values.

We begin by making a quantitative comparison of the present calculations with other relevant local-density-(LD) functional results for nitrogen. Our LD total energy for the isolated nitrogen pseudoatom E_{LD}^N is given in Table IV, along with the corresponding spin-polarized

TABLE IV. Total energies of selected equilibrium ($p=0$) nitrogen solids and isolated ($V = \infty$) nitrogen atoms and molecules. All energies are in eV/atom, exclude zero-point vibrational contributions, and are local-density (E_0 and E_{LD}), local-spin-density (E_{LSD}), or experimental (E_{expt}) results. The zero of energy is taken to be the LD equilibrium energy of the diatomic α-N_2 phase.

	Equilibrium solids		Isolated atoms or molecules	
N	E_0^{sc}	2.72	E_{LD}^N	8.89
	E_0^{cg}	0.97	E_{LSD}^N	5.85[a]
			E_{expt}^N	$E_{expt}^{N_2} + 4.95$[b]
N_2	$E_0^{\alpha N_2}$	0.0	$E_{LD}^{N_2}$	0.06
			$E_{expt}^{N_2}$	

[a]Reference 55.
[b]Reference 62.

energy E_{LSD}^N.[55] Note that both in this table and throughout the present work we take the zero of energy to be our LD calculated equilibrium energy for the α-N_2 phase of nitrogen, and we omit all zero-point contributions.[56] The difference $E_{coh}^{sc} = E_{LSD}^N - E_0^{sc} = 3.13$ eV/atom is our predicted cohesive energy for the sc phase of nitrogen, which may be compared with the value of 2.88 eV/atom obtained from linear muffin-tin orbital calculations using a different exchange-correlation potential.[15] A similar 0.2 eV/atom difference (8.63 vs 8.43 eV/atom) exists between E_{coh} values obtained in analogous LD calculations for diamond-phase carbon,[57,58] so that this agreement is consistent with differences due to exchange-correlation potentials and/or shape approximation effects (in Refs. 15 and 58). Another point of comparison is the dissociation energy $D_e = 2\,(E_{LSD}^N - E_{LD}^{N_2})$ of the N_2 molecule, where the factor of 2 is required since all of our total energies are given *per atom*. We also use our LD energy $E_{LD}^{N_2}$ here for the isolated pseudomolecule, as spin-polarization corrections should be unimportant for the approximately full shell configuration of the N_2 molecule. Our result for the dissociation energy of an isolated N_2 molecule is therefore $D_e = 11.58$ eV/molecule which may be compared to a recent augmented-plane-wave value of 11.5 eV/molecule.[59] Since the cohesive energy $E_{coh}^{\alpha N_2} = E_{LD}^{N_2} - E_0^{\alpha N_2}$ of the van der Waals bonded α-N_2 solid is quite small, the difference $\frac{1}{2}D_e - E_{coh}^{sc}$ provides a measure of the separation between our monatomic and diatomic curves. In this regard, our present results are seen to be in relatively close quantitative agreement with other LD calculations for nitrogen.

We now consider errors associated with the LD approximation itself. It is well known that such calculations overestimate the cohesive energies for certain classes of solids. The error is largest by far for second-period covalent nets,[2] about 1 eV/atom for both α-12 boron[60,61] and diamond-phase carbon,[57] and we expect a similar error for threefold-coordinated nitrogen. It is also generally believed that the error lies mostly with the local-spin-density (LSD) calculation of the atom in the case of such covalent nets, a belief which has been specifically confirmed by quantum Monte Carlo calculations in the case of diamond-phase carbon.[57] Moreover, the $p(V)$ equations of state and those bulk properties not involving the atom (V_0 and B_0) are generally in relatively good agreement with experiment for these materials, especially in contrast to van der Waals bonded molecular or rare-gas solids, as, for example, the argon results mentioned above.[53] We therefore believe our LD cg-N results in Fig. 6 to be accurate in compression, and that the significant LD (or LSD) errors occur at large expansion ($V \gg V_0^{cg} = 6.67$ Å^3/atom), culminating in an atom energy E_{LSD}^N which is ~ 1 eV higher than the true atom energy E_{expt}^N. In sharp contrast, the cohesive energy $E_{coh}^{\alpha N_2}$ of the diatomic solid is sufficiently small that LD errors in this quantity are unimportant. We obtain $E_{coh}^{\alpha N_2} = 0.06$ eV/atom, which may be compared to the adjusted experimental value of 0.08 eV/atom,[1] from which we have removed the zero-point contribution.[27] The significant diatomic LD errors are therefore more likely to appear in

compression, which is precisely the implication of the LD-experiment $p(V)$ comparison for ε-N_2 indicated in Fig. 5. Specifically, one may expect these diatomic errors in the range $3 \text{ Å}^3/\text{atom} < V < V_0^{\alpha N_2}$, since the inter- and intramolecular distances become comparable at the lower end of this range, at which point LD theory should be as accurate for the "diatomic" as for the polymeric or metallic phases.

There should be, and is, consistency between the monatomic and diatomic LD and LSD errors for nitrogen. Our semiempirical ε-N_2 equation of state (dashed curves in Figs. 5 and 6) has been constrained to equal our LD ε-N_2 results near $V \sim 3 \text{ Å}^3/\text{atom}$ (actually at $3.5 \text{ Å}^3/\text{atom}$ or 500 GPa) where we expect negligible LD errors in the difference $E^{cg}(V) - E^{\varepsilon N_2}(V)$. The total energy of this semiempirical equation of state is -0.43 eV/atom at equilibrium, which, given the experimental α-N_2 cohesive energy, provides the estimate $E_{\text{expt}}^{N_2} \sim -0.35$ eV/atom. This value in turn suggests $E_{\text{expt}}^{N} \sim 4.60$ eV/atom, based on the experimental dissociation energy of 9.90 eV/molecule,[62] and therefore a 1.25 eV/atom error in the LSD atom energy. This 1.25 eV/atom error is both consistent with the above-mentioned ~ 1 eV/atom E_{coh} errors for boron[60,61] and carbon,[57] and follows indications that it should be somewhat larger for the case of nitrogen.[63]

Turning to the consequence of these various errors on the transition pressure, we note first that the LD prediction (the common tangent sketched between the two solid curves in Fig. 6) is 33 GPa. If the diatomic result is replaced by our semiempirical ε-N_2 equation of state (dashed curve), the transition pressure is then 50 GPa. If the separation between these two curves (solid cg-N and dashed ε-N_2) is increased by a further 0.2 eV/atom, reflecting perhaps a larger error in E_{LSD}^{N} and/or a different diatomic structure with lower energy in the vicinity of $V = 8 \text{ Å}^3/\text{atom}$ in addition to zero-point energy corrections,[56] the transition pressure would increase to 65 GPa. In consideration of the above uncertainty analysis, we believe the most reliable value for the transition pressure to be 50 GPa, with uncertainties of about ±15 GPa.

The establishment of the equilibrium phase boundary between polymeric forms of nitrogen and the observed diatomic phases at relatively low pressure is one of the central results of the present theoretical study. The essential conclusion that the $N{\equiv}N$ triple bond will be destabilized at lower pressures than the $N{-}N$ single bond has also been suggested in previous theoretical work on high-pressure phases of nitrogen.[15,16] All theoretical analyses, including the present one, indicate that nitrogen should transform from its ambient diatomic form to an intermediate, yet still covalent, polymeric regime before losing its covalency altogether at still higher pressures. Two earlier calculations[15,16] have placed the transition to the polymeric regime at pressures below 100 GPa, the lower estimate being at 70 GPa.[16] Our predicted 50 ± 15 GPa transformation pressure is based on a polymeric structure which is significantly lower in energy than those previously considered;[15,16] however, we include for the first time estimates of errors in the diatomic equation of

state, which partially offset the reduction in pressure implied by the new lower-energy polymeric phase. Experimentally, diamond-anvil-cell experiments up to 130 and 180 GPa have suggested that nitrogen remains diatomic to these pressures at room temperature, however.[18,19] A possible explanation for the existence of diatomic nitrogen well above our predicted diatomic-to-polymeric transition pressure may be that the diatomic phase is itself metastable at these pressures. This explanation is not singular to the case of nitrogen. In fact, the graphite to diamond transition in carbon must be overdriven by about a factor of 7 in pressure even at a temperature of 1000 K.[20] Moreover, an anomaly has been seen above 30 GPa in *hot* shock compressed fluid nitrogen,[21] which has been interpreted as dissociation to a dense atomic phase,[22] and which is consistent with the theoretically predicted phase transition at low temperatures.[23]

IV. ATMOSPHERIC-PRESSURE METASTABILITY OF POLYMERIC NITROGEN

If diatomic nitrogen persists metastably at room temperature to pressures far above (by a factor of ~3) the equilibrium diatomic-polymeric phase boundary, such hysteresis raises the possibility that the polymeric form, once synthesized at high pressure, might also be metastable at atmospheric pressure. We now consider the prospects for atmospheric-pressure ($p \sim 0$) metastability of the cg, BP, and $A7$ polymeric phases of nitrogen discussed in the previous section. One may demonstrate mechanical stability of a given phase by showing that all phonon frequencies are real, which is equivalent to demonstrating a local minimum in the total-energy surface as a function of the atomic coordinates. For a structures such as cg or BP, with 4 atoms in the primitive cell and 12 modes at each point in the Brillouin zone, such calculations would be rather challenging for direct methods in which atoms are actually displaced,[64] so that a linear-response treatment would be more suitable.[65] Neither approach, however, would give barrier heights, a crucial parameter in any investigation of metastable lifetime.

We therefore follow a different approach, motivated by the collective aspect of martensitic transformations. Specifically, we identify transformation paths (described in the Appendix) between a polymeric phase and a lower-energy phase (either diatomic or polymeric), and then carry out *ab initio* pseudopotential total-energy calculations along such paths in order to determine potential barrier heights inhibiting the transformation. As in our previous work on carbon,[66] we use high-symmetry subgroups common to the space groups of the initial and final structures to help select the path. In addition, our experience with the carbon calculations has shown a direct correspondence with such calculated barrier heights and the number of bonds broken during the course of the transformation. Therefore, a realistic calculation of the barrier height requires paths which involve no unnecessary bond breaking. In regard to the potential instability of the atmospheric-pressure threefold-coordinated poly-

meric phases towards dimerization, for example, we seek paths which break only two of the bonds, with the third evolving continuously into the diatomic bond of the N_2 molecule. We have adopted such paths unless specifically indicated otherwise. In considering the dimerization of the polymeric phases, we have taken the simplest of the diatomic structures, the β-O_2 structure, in the case of BP and $A7$ initial structures, and a distortion of its two-layer variant (see Appendix and Table III) for cg, as the target phase. For convenience, we shall refer to the latter distortion of the two-layer variant as the "β'-O_2" structure. It is to be emphasized that we make no attempt to conclusively prove metastability, but are rather checking against the possibility of the kind of generic instability that is found, for example, in the high-coordination phases of carbon at atmospheric pressure.[66,67] We see no evidence for such behavior, and so our results are consistent with the possibility that each of the $A7$, BP, and cg polymeric phases may be metastable at atmospheric pressure.

The results of our stability analyses are indicated in Fig. 7 where the calculated total energy per atom is shown as a function of the reaction path describing the cg $\rightarrow$ β'-O_2, BP $\rightarrow$ β-O_2, and $A7$ $\rightarrow$ β-O_2 transformations. The cg $\rightarrow$ β'-O_2 transformation is mapped within the $P2_12_12_1$ space group and involves eight atoms per primitive cell (two sets of a sites). The BP $\rightarrow$ β-O_2 transformation is mapped within the $C2/m$ space group and

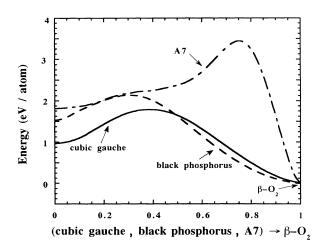(cubic gauche , black phosphorus , A7) $\rightarrow \beta$-O_2

FIG. 7. *Metastability of polymeric nitrogen.* Calculated total energy per atom as a function of the reaction coordinate for cg $\rightarrow$ β'-O_2 (solid line), BP $\rightarrow$ β-O_2 (dashed line), and $A7$ $\rightarrow$ β-O_2 (dash-dotted line) transformations, where β'-O_2 designates a distorted two-layer variant of the β-O_2 structure. Detailed characterization of these transformation paths is given in the Appendix. These are approximately zero-pressure paths, with the starting atomic volumes equal to the equilibrium values for the polymeric phases (6.67, 6.34, and 6.49 Å^3/atom for the cg, BP, and $A7$ phases, respectively), and the final volume the equilibrium value for the β-O_2 phase (19.67 Å^3/atom). A kinetic energy cutoff of $E_{cutoff} = 80$ Ry was used for all the calculations. The numbers of special **k** points used were 18, 32, and 10 for the cg, BP, and $A7$ transformations, respectively. The zero of energy corresponds to the diatomic β-O_2 structure.

involves four atoms per primitive cell (two sets of i sites). The $A7 \rightarrow$ β-O_2 transformation is mapped within the $R\bar{3}m$ space group and involves two atoms per primitive cell (one set of c sites). Along the transformation path, we define a transformation variable ξ which continuously evolves the structure from the initial polymeric phase ($\xi = 0$) to the final diatomic phase ($\xi = 1$). A *linear* transition path is defined by specifying the continuous functions of the variable ξ

$$
\begin{aligned}
\mathbf{a}(\xi) &= (1-\xi)\mathbf{a}^i + \xi\mathbf{a}^f, \\
\mathbf{b}(\xi) &= (1-\xi)\mathbf{b}^i + \xi\mathbf{b}^f, \\
\mathbf{c}(\xi) &= (1-\xi)\mathbf{c}^i + \xi\mathbf{c}^f, \\
x_1(\xi) &= (1-\xi)x_1^i + \xi x_1^f, \\
&\vdots \\
z_n(\xi) &= (1-\xi)z_n^i + \xi z_n^f,
\end{aligned} \tag{16}
$$

where the superscripts i and f indicate initial (cg, BP, or $A7$) and final (β-O_2 or β'-O_2) structures, and $\mathbf{a},\mathbf{b},\mathbf{c},x_1$, $\ldots$, z_n are the structural parameters appropriate to the space group of the transformation path ($P2_12_12_1$, $C2/m$, or $R\bar{3}m$). As described in the Appendix, our transformations for the cg and BP cases deviate somewhat from such linear paths in order that the three equal bond lengths in the initial polymeric phase evolve into only two unique lengths $d(\xi)$ and $d'(\xi)$ along the path, i.e., a shorter incipient N_2 bond length, and two equal longer "broken-bond" lengths. Our $A7$ path, on the other hand, is strictly linear, and all three bonds are broken during the course of the transformation, in that the final diatomic bond is formed between atoms which were not near neighbors at the start. This path is nevertheless of interest given that it is achieved without reduction in space-group symmetry, and is analogous to the *constant-volume* path investigated by Martin and Needs at a volume of 5 Å^3/atom.[16] Note that all of our transformation paths correspond to approximately *constant-pressure* transformations. More precisely, the initial and final structures correspond strictly to $p = 0$, while the intermediate structures given by Eq. (16), with modifications as specified in the Appendix, may be expected to be $p \sim 0$. Accordingly, the atomic volume varies along the transformation paths from the equilibrium volumes for the polymeric phases $V_{cg}^i = 6.67$ Å^3/atom, $V_{BP}^i = 6.34$ Å^3/atom, or $V_{A7}^i = 6.49$ Å^3/atom to the equilibrium volume for the diatomic phase $V_{\beta O_2}^f = 19.67$ Å^3/atom.

Inspection of Fig. 7 reveals that all three curves $E(\xi)$ exhibit positive curvature in the polymeric limit $\xi = 0$, indicating mechanical stability insofar as these modes are concerned. We have also verified that the curves rise in energy at small negative values of ξ, which corresponds to the formation of chains in the case of the cg and BP paths. These results are therefore consistent with the atmospheric-pressure stability of the cg and BP phases of polymeric nitrogen against either N$\equiv$N dimerization or the formation of N$-$N$=$N chains, albeit demonstrated here only for select, but physically natural, paths. The actual barrier heights are ΔE_b(cg $\rightarrow$ β'-O_2) ≈ 0.86

eV/atom and $\Delta E_b(\text{BP} \to \beta\text{-O}_2) \approx 0.59$ eV/atom, which may be viewed as the energy required to break two bonds at each N atom followed by their reconstitution as part of the new triple bond in the remaining bond direction. For the $A7$ path, on the other hand, the three near-neighbor distances change but remain equal for increasing ξ, until for $\xi \sim 0.75$ a new neighbor becomes the closest. This observation is in good correspondence with the previous constant-volume work indicating that the maximum energy along this path occurs at this point of approximate fourfold coordination.[16] In our case $(p \sim 0)$ this leads to a barrier $\Delta E_b(A7 \to \beta\text{-O}_2) \approx 1.65$ eV/atom, which reflects three broken bonds, and is therefore expected to be higher than the other two barriers cited.

We have also considered possible paths between the three polymeric phases. The $A7$ and BP structures are both corrugated double layers, as discussed in Sec. III. An $A7 \to$ BP transformation requires either bond breaking or bending. In the first case, one may imagine reassembling the $A7$ double layers to form something like the sc parent, which may then be separated into new BP-like double layers parallel to one of the sc [100] directions. The barrier would be roughly the sc–$A7$ energy difference of Table I, or about 0.9 eV/atom. In the second case, one may change the topology of the individual corrugated double layers by bending bonds, as may be accomplished within the $C2/m$ subgroup of the two structures (two sets of $4i$ sites per unit cell). We have performed calculations along such a path and found a barrier $\Delta E_b(A7 \to \text{BP}) \approx 0.36$ eV/atom (32 special k-point samplings). These numbers are consistent with the expectation that bond breaking should be more energetically costly than bond bending. With this in mind, it is to be noted that the bond breaking followed by rebonding is essential for any path between the $A7$ or BP structures and the fully three-dimensional covalent net exhibited by the cg phase of nitrogen. We therefore expect significant barriers inhibiting any $A7 \to$ cg or BP $\to$ cg transformations.

The present metastability calculations are clearly limited and certainly not conclusive. Yet it is to be emphasized that we see no evidence for mechanical instabilities in any of the polymeric phases of nitrogen at atmospheric pressure, and instead, rather large energy barriers inhibiting transformations from one to another as well as to lower-energy diatomic forms. In particular, we note the 0.86 eV/atom barrier inhibiting dimerization of the atmospheric-pressure cg phase. Moreover, it is possible on the basis of these results to rule out the kind of generic instability which is seen in theoretical calculations for high-coordination structures of atmospheric pressure carbon.[66,67]

V. SUMMARY

Results of *ab initio* pseudopotential total-energy calculations indicate that the equilibrium phase boundary between single-bonded, threefold-coordinated polymeric forms of nitrogen, and the observed, triple-bonded diatomic phases may occur at relatively low pressure, 50 ± 15 GPa. This observation is based on the identifi-

cation of low-energy polymeric phases of nitrogen, calculation of their equations of state, and on an *ab initio* pseudopotential calculation of the equation of state for the observed high-pressure $\varepsilon\text{-N}_2$ diatomic phase. Most important among these polymeric nitrogen phases are the black-phosphorus structure and a cubic phase characterized by the occurrence of all-*gauche* dihedral angles. The latter cubic *gauche* (cg) structure was found to be the lowest-energy modification among atomic forms of nitrogen, and we locate its minimum energy 0.86 eV/atom below the previously investigated[16] arsenic $(A7)$ phase. The $\varepsilon\text{-N}_2$ structure was found to have the lowest energy among the diatomic phases considered at modest compression, in agreement with experiment. Moreover, we have estimated the local-density-functional errors in these results based on a comparison of the present and related theoretical results with available experimental data for both nitrogen itself, as well as for other materials whose bonding is similar to either the polymeric or diatomic phases of nitrogen. These considerations are incorporated into our predicted $\varepsilon\text{-N}_2 \to$ cg-N transition pressure of 50 ± 15 GPa, a modest pressure on the scale of present diamond-anvil-cell capabilities.

We believe the diatomic form of nitrogen that has been observed at room temperature and pressures up to 180 GPa,[18,19] to be metastable at these conditions. Such hysteresis raises the prospect that a polymeric form of nitrogen, if synthesized at high pressure, might also be metastable at atmospheric pressure. With this possibility in mind, we have carried out total-energy calculations along selected transformation paths between various polymeric phases, and from these to a simple, lower-energy diatomic phase. In all cases we find significant barriers inhibiting these transformations, and in particular, a $\sim$0.9 eV/atom barrier inhibiting dimerization of the cg polymeric form of nitrogen at atmospheric pressure. While by no means compelling, these results are certainly consistent with the existence of a metastable polymeric form of nitrogen at atmospheric pressure.

Note added in proof. Recent room-temperature x-ray diffraction measurements on compressed diatomic nitrogen to 44 GPa [H. Olijnyk, J. Chem. Phys. **93**, 8968 (1990)] yield a $p(V)$ curve within ±2 GPa of our semiempirical result in Fig. 6, while Raman data [H. Schneider, W. Häfner, A. Wokaun, and H. Olijnyk, J. Chem. Phys. **96**, 8046 (1992); are consistent with a diatomic phase which is still only a slight distortion of the $R\bar{3}c$ $\varepsilon\text{-N}_2$ structure at 54 GPa. Quantum Monte Carlo calculations [L. Mitas and R. M. Martin (private communication)] also suggest a larger LSD error for the total energy of the nitrogen atom than our 1.25-eV estimate of Sec. III E. If there are no compensating LD errors in the equilibrium total energy of the cg phase, this would lead to a larger $\varepsilon\text{-N}_2 \to$cg transition pressure than predicted here.

ACKNOWLEDGMENTS

Munitions Technology Development Program. We gratefully acknowledge conversations with R. LeSar, R. M. Martin, D. Schiferl, and M. van Schilfgaarde.

APPENDIX

In this appendix, we provide a brief description of the $cg \rightarrow \beta'\text{-}O_2$, $BP \rightarrow \beta\text{-}O_2$, and $A7 \rightarrow \beta\text{-}O_2$ transformation paths used in our metastability calculations of Sec. IV, where "$\beta'\text{-}O_2$" designates a distortion of the two-layer variant of $\beta\text{-}O_2$ indicated in Table III. These structural transformations involve the continuous distortion of one structure into another, and consequently, can be described as martensitic. As in previous work on carbon,[66] we have used high-symmetry subgroups of the initial and final space groups in order to aid selection of these paths. In addition, we generally seek paths without unnecessary bond breaking, so that in dimerization of the threefold coordinated polymeric phases, one of the three bonds should continuously evolve into the diatomic bond of the final structure. These paths are also linear in the sense of Eq. (16), or nearly linear as will be discussed for the cg and BP cases, where the structural parameters $a(\xi),b(\xi),c(\xi),x_1(\xi),\dots,z_n(\xi)$ pertain to the space group of the transformation path, i.e., the appropriate subgroup of the space groups of the initial and final structures.

1. Cubic *gauche* (cg) $\rightarrow \beta'\text{-}O_2$ transformation

Common subgroups of the cg and $\beta\text{-}O_2$ structures are of relatively low symmetry, so that we consider first the target structure in this case to be the two-layer variant of $\beta\text{-}O_2$ in Table III. The mapping is accomplished by means of the $P2_12_12_1$ space group with a primitive orthorhombic Bravais lattice and eight atoms per primitive cell (two sets of a sites). The conventional unit cell is primitive, with $a_0(\xi) = a(\xi) = a(\xi)\,\hat{x}$, $b_0(\xi) = b(\xi) = b(\xi)\,\hat{y}$, and $c_0(\xi) = c(\xi) = c(\xi)\,\hat{z}$, in terms of which the $4a$ sites are

$$[x(\xi), y(\xi), z(\xi)]\,, \quad [\tfrac{1}{2} - x(\xi),\ -y(\xi),\ \tfrac{1}{2} + z(\xi)]\,,$$
(A1)
$$[-x(\xi),\ \tfrac{1}{2} + y(\xi),\ \tfrac{1}{2} - z(\xi)]\,, \quad [\tfrac{1}{2} + x(\xi),\ \tfrac{1}{2} - y(\xi),\ -z(\xi)].$$

The initial ($\xi = 0$) and terminal ($\xi = 1$) values of (a, b, c, x_1, y_1, z_1, x_2, y_2, z_2) are

$$(a_{cg}, a_{cg}, a_{cg}, x_{cg}, x_{cg}, x_{cg}, \tfrac{1}{2} + x_{cg}, \tfrac{1}{2} + x_{cg}, \tfrac{1}{2} + x_{cg})\,,$$
(A2a)
$$(a_{\beta'O_2}, b_{\beta'O_2}, c_{\beta'O_2}, \tfrac{1}{4}, y_{\beta'O_2}, z_{\beta'O_2}, \tfrac{3}{4}, \tfrac{1}{2} - y_{\beta'O_2},$$
$$\tfrac{1}{2} + z_{\beta'O_2}),$$
(A2b)

respectively. The values of these parameters may be obtained from Tables I–III, where the two-layer $\beta\text{-}O_2$ values are to be used for $\beta'\text{-}O_2$ parameters. The end points given by Eq. (A2) are schematically illustrated in Fig. 8.

Our barrier-height calculations in Fig. 7 utilize a slight modification of the linear path defined by Eqs. (16) and (A2). We retain the linear evolution in these equations for $a(\xi)$, $b(\xi)$, $c(\xi)$, $y_1(\xi)$, $z_1(\xi)$, $y_2(\xi)$, and $z_2(\xi)$, how-
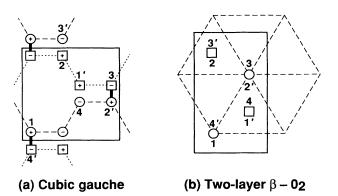

(a) Cubic gauche   **(b) Two-layer $\beta - O_2$**

FIG. 8. *Cubic gauche* $\rightarrow$ $\beta'\text{-}O_2$ *transformation.* Schematic illustration of the relation between (a) the cubic *gauche* (cg) and (b) the two-layer $\beta\text{-}O_2$ structure which permits one to be mapped into the other by the $P2_12_12_1$ space group with two sets of $4a$ sites. The diagrams show cross sections of the unit cell perpendicular to the c axes. Circles and squares signify atoms associated with different planes, $0c$ and $\tfrac{1}{2}c$ for (a), $\tfrac{1}{4}c$ and $\tfrac{3}{4}c$ for (b), respectively, while the $\pm$ signs indicate positions slightly above or below these planes. The bold, dashed, and dotted lines in (a) indicate bonds in the cg phase, with the bold lines evolving into the diatomic bonds in (b). The diatomic axes in (b) are parallel to the c axis, while the lateral packing of the molecules is hexagonal (dashed lines).

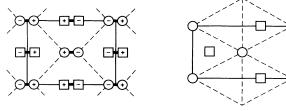ever, and we determine $x_1(\xi)$ and $x_2(\xi)$ from

$$x_1(\xi) = \tfrac{1}{8} - \tfrac{1}{2}[\ \tfrac{3}{4} + 4y_1(\xi)y_2(\xi) - 3y_1(\xi)$$
$$-y_2(\xi)]\left(\frac{b(\xi)}{a(\xi)}\right)^2 + 2z_1(\xi)^2\left(\frac{c(\xi)}{a(\xi)}\right)^2,$$
(A3a)
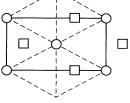$$x_2(\xi) = x_1(\xi) + \tfrac{1}{2}\,.$$
(A3b)

The resultant path provides a relatively symmetric and monotonic splitting of the single bond length at the polymeric limit into just two unique lengths $d(\xi)$ and $d'(\xi)$ along the path, i.e., a shorter incipient N_2 bond length, and two equal longer "broken-bond" lengths. The $\xi = 1$ end point of this path is a slight $P2_12_12_1$ distortion of the two-layer $\beta\text{-}O_2$ variant, which we designate as $\beta'\text{-}O_2$ for convenience.

2. Black-phosphorus (BP) $\rightarrow \beta\text{-}O_2$ transformation

Although there are three bonds of essentially equal length connecting each atom in the BP structure, the one *trans* bond is not required by symmetry to have exactly the same length as the two equal *gauche* bonds, and is therefore the natural candidate for evolution into the diatomic bond in any potential dimerization of the BP structure. Assuming this constraint, and the target diatomic phase to be the $\beta\text{-}O_2$ structure for convenience, a relatively high-symmetry path is provided within the $C2/m$ space group. The corresponding structure has a monoclinic Bravais lattice with four atoms per primitive cell (two sets of i sites). The unit cell vectors may be written $a(\xi) = a(\xi)\,\hat{x}$, $b(\xi) = b(\xi)\,\hat{y}$,

(a) Black phosphorus   **(b) β − 0₂**

FIG. 9. *Black-phosphorus* → *β-O₂ transformation.* Schematic illustration of the relation between (a) the black-phosphorus (BP) and (b) the β-O_2 structure which permits one to be mapped into the other by the $C2/m$ space group with two sets of $4i$ sites per unit cell. These diagrams show cross sections of the unit cell parallel to the $\mathbf{a}$,$\mathbf{b}$ plane, with circles and squares signifying atoms associated with two neighboring layers at different heights, and the $\pm$ signs indicating atom positions slightly above or below these planes. The bold and dashed lines in (a) show the bonding in one such corrugated double layer of the BP structure, with the former bonds evolving into the diatomic bonds in the diatomic limit (b). The diatomic axes in (b) are perpendicular to the $\mathbf{a}$,$\mathbf{b}$ plane, with hexagonal packing in the plane indicated by the dashed lines. The monoclinic shear in this transformation is evident from the higher layer of atoms (squares), which appear shifted to the right in (b) relative to the lower layers (circles).

and $\mathbf{c}(\xi) = c_x(\xi)\,\hat{\mathbf{x}} + c_z(\xi)\,\hat{\mathbf{z}}$, in terms of which [recall Eq. (1)] the two i sites associated with the primitive cell are $\pm[x(\xi), 0, z(\xi)]$, while the primitive cell vectors may be taken

$$(1,\ 0,\ 0),\quad (0,\ \tfrac{1}{2},\ \tfrac{1}{2}),\quad (0,0,1)\ . \tag{A4}$$

We have used the $A12/m1$ setting of the $C2/m$ space group, with unique axis $\mathbf{b}$.[41] The initial ($\xi = 0$) and terminal ($\xi = 1$) values of $(a,\ b,\ c_x,\ c_z,\ x_1,\ z_1,\ x_2,\ z_2)$ are

$$(c_{BP}, a_{BP}, 0, b_{BP}, z_{BP}, y_{BP}, \tfrac{1}{2} - z_{BP}, \tfrac{1}{2} + y_{BP}), \tag{A5a}$$

$$(\sqrt{3}\ a_{\beta O_2}, a_{\beta O_2}, a_{\beta O_2}/\sqrt{3}, \tfrac{2}{3}c_{\beta O_2}, -\tfrac{1}{2}z_{\beta O_2},$$

$$\tfrac{3}{2}z_{\beta O_2}, \tfrac{1}{2} - \tfrac{1}{2}z_{\beta O_2}, \tfrac{1}{2} + \tfrac{3}{2}z_{\beta O_2}), \tag{A5b}$$

respectively, where the values of these parameters may be obtained from Tables I–III. The two end points of this transformation given by Eq. (A5) are schematically illustrated in Fig. 9.

As with the cg mapping, a simple adjustment to the linear path specified by Eqs. (16) and (A5) provides for a relatively symmetric and monotonic splitting of the single bond length in the BP limit into just two unique lengths along the path, a shorter incipient N_2 bond length, and two equal longer "broken-bond" lengths. The adjustment is made only to $x_2(\xi)$,

$$x_2(\xi) = \tfrac{1}{2} - x_1(\xi) - 2z_1(\xi)\frac{\mathbf{a}(\xi)\cdot\mathbf{c}(\xi)}{a(\xi)^2} \tag{A6}$$

with all other structural parameters taken from the linear mapping. This modification has no impact on the initial or final structures, which are still precisely BP and β-O_2, and has been used in the barrier height calculations in Fig. 7.

3. Arsenic ($A7$) → β-O_2 transformation

The $A7$ and β-O_2 structures both belong to the same $R\bar{3}m$ space group and are characterized by the same c site positions. Consequently, a trivial $A7 \to \beta$-O_2 transformation exists simply by continuously varying the values of the two lattice constants and the one internal parameter. Specifically, the transformation is described by Eqs. (2) and (3), with the three structural parameters $a(\xi)$, $c(\xi)$, and $z(\xi)$ varying from the $A7$ values at $\xi = 0$ to the β-O_2 values at $\xi = 1$. This transformation does not evolve one of the three bonds connecting each atom in the $A7$ structure into the diatomic bond in the β-O_2 structure. Rather, the three bonds stay equal in length, with a new neighbor eventually moving closer and receiving the diatomic bond.

[1] D. A. Young, *Phase Diagrams of the Elements* (University of California Press, Berkeley, 1991).

[2] A. F. Wells, *Structural Inorganic Chemistry*, 5th ed. (Clarendon, Oxford, 1984),

[3] R. J. Bartlett, W. J. Lauderdale, J. F. Stanton, J. Gauss, and K. Ferris (unpublished).

[4] P. Saxe and H. F. Schaefer III, J. Am. Chem. Soc. **105**, 1760 (1983).

[5] H. Huber, T.-K. Ha, and M. T. Nguyen, J. Mol. Struct. (Theochem.) **105**, 351 (1983).

[6] M. Ramek, J. Mol. Struct. (Theochem.) **109**, 391 (1984).

[7] R. Engelke, J. Phys. Chem. **93**, 5722 1989).

[8] R. Engelke and J. R. Stine, J. Phys. Chem. **94**, 5689 (1990).

[9] D. H. Magers, E. A. Salter, R. J. Bartlett, C. Salter, B. A. Hess, Jr., and L. J. Schaad, J. Am. Chem. Soc. **110**, 3435 (1988).

[10] A. Vogler, R. E. Wright, and H. Kunkely, Angew. Chem., Int. Ed. Engl. **19**, 717 (1980).

[11] Y. Kim, J. W. Gilje, and K. Seff, J. Am. Chem. Soc. **99**, 7057 (1977).

[12] A. K. McMahan, Physica B+C **139&140B**, 31 (1986).

[13] K. Takemura, S. Minomura, O. Shimomura, and Y. Fujii, Phys. Rev. Lett. **45**, 1881 (1980); Y. Fujii, K. Hase, N. Hamaya, Y. Ohishi, A. Onodera, O. Shimomura, and K. Takemura, *ibid.* **58**, 796 (1987).

[14] I. F. Silvera, in *Simple Molecular Systems at Very High Density*, edited by A. Polian, P. Loubeyre, and N. Boccara (Plenum, New York, 1989).

[15] A. K. McMahan and R. LeSar, Phys. Rev. Lett. **54**, 1929 (1985).

[16] R. M. Martin and R. J. Needs, Phys. Rev. B **34**, 5082 (1986).

[17] A. K. McMahan, Int. J. Quan. Chem.: Quan. Chem. Symp. **20**, 393 (1986).

[18] R. Reichlin, D. Schiferl, S. Martin, C. Vanderborgh, and R. L. Mills, Phys. Rev. Lett. **55**, 1464 (1985).

[19] P. M. Bell, H. K. Mao, and R. J. Hemley, Physica B+C **139&140B**, 16 (1986).

[20] See Fig. 10 in F. P. Bundy, J. Geophys. Res. **85**, 6930 (1980).

[21]H. B. Radousky, W. J. Nellis, M. Ross, D. C. Hamilton, and A. C. Mitchell, Phys. Rev. Lett. **57**, 2419 (1986).

[22]M. Ross, J. Chem. Phys. **86**, 7110 (1987).

[23]D. C. Hamilton and F. H. Ree, J. Chem. Phys. **90**, 4972 (1989).

[24]L. Radom, J. Baker, P. M. W. Gill, R. H. Nobes, and N. V. Riggs, J. Mol. Struct. **126**, 271 (1985).

[25]D. Schiferl, S. Buchsbaum, and R. L. Mills, J. Phys. Chem. **89**, 2324 (1985).

[26]R. L. Mills, B. Olinger, and D. T. Cromer, J. Chem. Phys. **84**, 2837 (1986).

[27]R. LeSar, J. Chem. Phys. **81**, 5104 (1984).

[28]C. A. English and J. A. Venables, Proc. R. Soc. London, Ser. A **340**, 57 (1974).

[29]See, for example, *Theory of the Inhomogeneous Electron Gas*, edited by S. Lundqvist and N. M. March (Plenum, New York, 1983).

[30]J. Ihm, A. Zunger, and M. L. Cohen, J. Phys. C **12**, 4409 (1979); **13**, 3095(E) (1980).

[31]W. E. Pickett, Comput. Phys. Rep. **9**, 115 (1989).

[32]D. R. Hamann, M. Schlüter, and C. Chiang, Phys. Rev. Lett. **43**, 1494 (1979).

[33]L. Kleinman and D. M. Bylander, Phys. Rev. Lett. **48**, 1425 (1982).

[34]N. Trouiller and J. L. Martins, Phys. Rev. B **43**, 1993 (1991).

[35]D. M. Ceperley and B. J. Alder, Phys. Rev. Lett. **45**, 566 (1980).

[36]J. Perdew and A. Zunger, Phys. Rev. B **23**, 5048 (1981).

[37]O. H. Nielsen and R. M. Martin, Phys. Rev. Lett. **50**, 697 (1983).

[38]H. J. Monkhorst and J. D. Pack, Phys. Rev. B **13**, 5188 (1976).

[39]The number of special **k** points used for the various phases were face-centered cubic (28), body-centered cubic (26), ideal hexagonal close packed (36), simple cubic (20), cubic diamond (28), arsenic $A7$ (28), black phosphorus (16), cubic *gauche* (18), chainlike (16), α-N$_2$ (11), ε-N$_2$ (2 and 10 in tests), and β-O$_2$ (10).

[40]M. P. Teter, M. C. Payne, and D. C. Allan, Phys. Rev. B **40**, 12255 (1989).

[41]*International Tables for Crystallography*, edited by Theo Hahn, 2nd ed. (Kluwer Academic, Dordrecht, 1989), Vol. A.

[42]F. D. Murnaghan, Proc. Natl. Acad. Sci. U.S.A. **30**, 244 (1944).

[43]M. H. Cohen, L. M. Falicov, and S. Golin, IBM J. Res. Dev. **8**, 215 (1964).

[44]T. Kikegawa and H. Hiwasaki, J. Phys. Soc. Jpn. **56**, 3417 (1987).

[45]H. J. Beister, K. Strössner, and K. Syassen, Phys. Rev. B **41**, 5535 (1990).

[46]T. Kikegawa and H. Hiwasaki, Acta Crystallogr. B **39**, 158 (1983).

[47]M. Okajima, S. Endo, Y. Akahama, and S. Narita, Jpn. J. Appl. Phys. **23**, 15 (1984).

[48]J. Donohue, *The Structures of the Elements* (Wiley, New York, 1974)

[49]A. F. Schuch and R. L. Mills, J. Chem. Phys. **52**, 6000 (1970).

[50]D. T. Cromer, R. L. Mills, D. Schiferl, and L. A. Schwalbe, Acta Crystallogr. B **37**, 8 (1981).

[51]We used ε-N$_2$ structural parameters appropriate for a pressure of 75 GPa, which differ from those at 10 GPa in Ta-

ble IV of Ref. 27 only in the slight increase of the rhombohedral angle α from 84.97° to 85.72°. R. LeSar (private communication).

[52]T. A. Scott, Phys. Rep. **27**, 89 (1976).

[53]A. K. McMahan, Phys. Rev. B **33**, 5344 (1986). Equation of state results for $T = 0$ fcc argon obtained (although not reported) in this work included equilibrium volume $V_0 = 28.45$ Å^3/atom, bulk modulus $B_0 = 8.4$ GPa, and cohesive energy $E_{\rm coh} = 0.07$ eV/atom, which may be compared to experimental values (Ref. 1) $V_0 = 35.96$ Å^3/atom, $B_0 = 2.86$ GPa, and $E_{\rm coh} = 0.089$ eV/atom, where estimates of zero-point contributions (4% in V_0, 0.009 eV/atom in $E_{\rm coh}$) have been removed from the latter.

[54]M. Ross, H. K. Mao, P. M. Bell, and J. A. Xu, J. Chem. Phys. **85**, 1028 (1986).

[55]The spin-polarization reduction in the energy of the nitrogen atom $E_{\rm LDA}^{\rm N} - E_{\rm LSDA}^{\rm N} = 3.04$ eV, as obtained from local-spin-density approximate calculations using the Ceperley-Alder exchange-correlation potential (Ref. 35). M. van Schilfgaarde (private communication).

[56]A Debye model was used to evaluate the zero-point energy contribution $E_{\rm zp} = (\frac{9}{8})\hbar\omega_D$, where ω_D is the Debye frequency. This leads to a zero-point energy correction in the polymeric cubic *gauche* phase of $E_{\rm zp}^{\rm cg-N} = 0.152$ eV/atom and an intermolecular zero-point energy correction in the molecular α-N$_2$ phase of $E_{\rm zp}^{\alpha\text{-}\rm N_2}({\rm inter}) = 0.007$ eV/atom. The intramolecular zero-point energy correction in the molecular α-N$_2$ phase may be obtained from Ref. 62 (pp. 412–420) and is equal to $E_{\rm zp}^{\alpha\text{-}\rm N_2}({\rm intra}) = 0.073$ eV/atom, leading to a total zero-point energy correction of $E_{\rm zp}^{\alpha\text{-}\rm N_2} = E_{\rm zp}^{\alpha\text{-}\rm N_2}({\rm inter}) + E_{\rm zp}^{\alpha\text{-}\rm N_2}({\rm intra}) = 0.007 + 0.073 = 0.080$ eV/atom. Consequently, the total difference in zero-point energy corrections between the polymeric and molecular nitrogen phases at zero pressure is estimated to be $\Delta E_{\rm zp}(p = 0) = 0.072$ eV/atom.

[57]S. Fahy, X. W. Wang, and S. G. Louie, Phys. Rev. Lett. **61**, 1631 (1988); Phys. Rev. B **42**, 3503 (1990).

[58]A. K. McMahan, Phys. Rev. B **30**, 5835 (1984).

[59]J. M. Soler and A. R. Williams, Phys. Rev. B **42**, 9728 (1990).

[60]S. Lee, D. M. Bylander, and L. Kleinman, Phys. Rev. B **42**, 1316 (1990).

[61]C. Mailhiot, J. B. Grant, and A. K. McMahan, Phys. Rev. B **42**, 9033 (1990).

[62]K. P. Huber and G. Herzberg, *Molecular Spectra and Molecular Structure* (Van Nostrand, New York, 1979), Vol. IV.

[63]J. A. Moriarty, Phys. Rev. B **19**, 609 (1979); (private communication). The difference between Moriarty's valence energy [corrected for spin polarization, V. L. Moruzzi, J. F. Janak, and A. R. Williams, *Calculated Electronic Properties of Metals* (Pergamon, New York, 1978)] and the appropriate sum of experimental ionization potentials is 0.67, 0.93, and 1.48 eV for the boron, carbon, and nitrogen atoms, respectively.

[64]See, e.g., R. M. Martin, in *Electronic Structure, Dynamics, and Quantum Structural Properties of Condensed Matter*, edited by J. DeVreese (Plenum, New York, 1985), p. 175.

[65]S. Baroni, P. Gianozzi, and A. Testa, Phys. Rev. Lett. **58**, 1861 (1987); **59**, 2662 (1987).

[66]C. Mailhiot and A. K. McMahan, Phys. Rev. B **44**, 11578 (1991).

[67]S. Fahy and S. G. Louie, Phys. Rev. B **36**, 3373 (1987); S. Fahy, S. G. Louie, and M. L. Cohen, *ibid.* **34**, 1191 (1986); **35**, 7623 (1987).